Proceedings of the International Gas Turbine Congress 2003 Tokyo
November 2-7, 2003

Bird Impact Analysis of Pre-Stressed Fan Blades Using Explicit Finite Element Code

Rajeev Jain and K. Ramachandra

Gas Turbine Research Establishment
Bangalore-560 093 (INDIA)
Email: rajeevjain@mail.gtre.org

ABSTRACT

This paper demonstrates use of explicit finite element code to predict blade damage caused due to 0.9 kg bird mass at critical flight velocity. Bird model is considered as hydrodynamic with length to diameter ratio of two. This paper also indicates failure of centrifugal stiffened blades using forming limit diagram and radial unbalance and axial force on engine bearing due to transient impact forces.

NOMENCLATURE

Compressibility ratio	μ
Poisson's ratio	ν
Density	ρ
Yield stress	σ_y
Young's Modulus	E
Hardening Modulus	E_h
Bulk Modulus	K
Blade tip radius from axis of rotation	R

INTRODUCTION

One of the major hazards to flight safety today is the in-flight impact of birds. Many external aircraft components of an aircraft such as windshield, fuselage and nose cone and engine components such as bullet-nose, inlet-strut, and rotating and stationary blades are susceptible to collisions with birds. Aircraft windshields and engine blades are especially vulnerable to damage. Airworthiness standards require that these critical components should be capable of withstanding bird strikes at critical flight speed to a certain degree. All gas turbine engines are designed to be safe and durable in order to withstand bird ingestion incidence.

Major factors affecting the structural response of fan blades under a bird strike are bird size (weight), blade size, bird velocity, fan blade rotational speed, fan blade span wise location of impact, and bird orientation with respect to engine centerline. Forcing function of bird impact loading times is typically in the range of milli-second.

A lot of work has been carried out to predict bird behavior during impact. Peterson and Barber (1976) concluded that, for impact velocities associated with bird strikes on aircraft and turbo-machinery. Birds behave like a fluid during impact. Later, Barber et al. (1977) conducted real bird impact tests on rigid targets and showed that bird-loading model treats the bird model as a fluid dynamic process. They also found that peak pressures generated during impact are independent of bird size but are proportional to square of velocity of the bird.

It is very difficult to conduct real bird-impact tests against aircraft components. A lot of work has been carried out to determine prime constituents of substitute bird model. Allcock and Collin (1968) studied wax, foam, emulsions, and gelatin as substitute materials for birds. They concluded that the soft material substitutes with specific gravities of water produced loading profiles similar to birds. Wilbeck and Rand (1981) tested various dummy bird substitutes and found that gelatin, with the specific gravity of water, produced loading profile similar to real birds. It has also been found that bird projectile response depends on material density and not on material strength.

In studying the bird impact response on aircraft structure, velocity of stationary components is determined by the velocity of aircraft, which in the case of military aircraft may be in the sonic range in low-level flight. In rotating engine components, the relative speed between bird and component depends on the speed of revolution. For this reason, the damage on rotating components is more extensive at medium aircraft speed and is defined as critical speed. Jain (2000) showed analytically that critical speed of a typical bladed disc assembly lies in between 120 to 140 m/sec.

Local structure response is strongly coupled to the overall deformation of the structure. The gross structural response is dominated by the low-

Manuscript Received on March 31, 2003

frequency components of the model spectrum. In the case of a small un-shrouded fan blade, first torsion and first bending dominate the dynamic structural response under medium or large bird impact loading. Cornell (1976) developed a theoretical analysis, which defines the loading and response of a rotor fan blade due to soft or frangible impacts in terms of three fundamental modes of vibration by representing the blade as a lumped, spring mass system. Storace et al. (1983) used transient structural analysis computer program NONSAPM for predicting nonlinear response and damage due to bird ingestion. Martin (1990) used transient dynamic analysis code WHAM using spherically shaped fluid finite elements as a soft body impactor shape. Niering (1990) used DYNA3D code to predict bird impact response on static blade. Later, Teichman and Tadros (1991) used PW/WHAM to simulate the behaviour of small fan blades subjected to bird impact loading.

In this paper the use of commercially available explicit finite element hydrodynamic couple code, MSC-DYTRAN (1992) to predict centrifugally stiffened blade response due to bird impact is discussed. Failure of blades is predicted by comparing major and minor strain against forming limit diagram. This paper also highlights the necessary inputs obtained from this analysis i.e. axial and radial unbalance loads for designing axial thrust bearing.

DESIGN METHODOLOGY

As per design philosophy for fan blades, few of the design criteria are laid down as follows:

1. Limit local plastic deformation to a specific percentage of chord to avoid stall/surge.
2. Limit strains in the impact region in order to avoid tearing and mass loss.
3. Limit strains at the root of the blade in order to prevent airfoil loss
4. Limit displacements in order to avoid contact with adjacent blades and stages.

In this investigation damage variables addressed include surface principal strains, local plastic deformation such as bulging, and overall blade displacements resulting from far field structural response. The surface maximum and minimum principal strains are used in conjunction with a forming limit concept whereby the relative values of these strains are compared to a failure boundary or forming limit diagram (FLD) to establish no tearing and possible mass loss occurs.

FINITE ELEMENT MODEL

Finite element model of first stage fan disk with twenty-four blades was created using I-DEAS and in-house software BMODE. Figure 1 shows finite element model of bladed disc geometry with Eulerian mesh. Disc geometry is approximated using uniform thickness shell elements whereas variable thickness shell elements are used for blade geometry. It is also assumed that blade is fixed rigidly with the disc and dowel root of the disc and dowel pins are not created to reduce number of elements for the analysis.

Blade Model

Bladed disc assembly of Fan disc finite element model consists of 8,520 nodes and 7,920 Belytschko-Tsay shell elements. Since the thickness of blade varies from tip to bottom as well as from leading edge to trailing edge, variable thickness shell elements are used to create finite element model of blades.

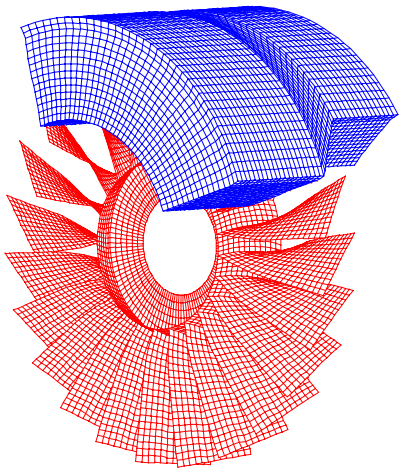

Figure 1 Lagrangian and Eulerian mesh for bird impact analysis

Bird Model

Bird is defined in Euler space as a cylindrical projectile by describing radius and end coordinates of the cylinder. Initial velocity of the bird is taken as 140 m/sec with length to diameter ratio nearly 2. Density of the bird projectile is taken as 1000 kg/m^3 with length and diameter of 166 and 84 mm respectively. Euler mesh in which cylindrical projectile of bird is defined consists of 25,380 solid brick elements and 28,416 nodes.

Contact Algorithm

At the interface of Lagrange (blade) and Euler mesh, Arbitrary-Lagrange-Euler coupling is defined. Also, contact is defined between adjacent blades of bladed disc assembly to simulate real bird impact situation.

FINITE ELEMENT ANALYSIS

There are twenty-four blades in rotor assembly to be analysed for bird impact analysis. Rim and bore radius of rotor disc are 0.33R and 0.22R respectively

where R is blade tip distance from axis of rotation (Figure 2). Bird impact location is at 0.9R distance from the axis of rotation.

Bird impact analysis on rotating blades is carried out in three phases i.e. displacement extraction, dynamic relaxation and impact phase. Since, centrifugal rotation leads to significant deformation, geometrical non-linear analysis is carried out around 11000 rpm to obtain initial displacements using implicit finite element code (MSC-NASTRAN).

Pre-stress Analysis

Initial displacements from non-linear FEM analysis are used as a necessary input to carry out pre-stress analysis. Stresses are stabilized after providing damping parameter. Pre-stress analysis using explicit code showed identical stress pattern as observed after implicit analysis. Further check has been done after comparing maximum deflection at the tip of the blade using non-linear implicit code with stablised deflection in time history plot. Figure 2 shows location of the bird before impact.

Bird Impact Analysis

The blade model rotation during impact is simulated by rigidly constraining the hub of the disc to rotate at a specified constant speed while all other nodes are given the corresponding initial steady state centrifugal velocity. The prescribed initial displacement vector and initial blade velocity measure blade centrifugal stiffening and equilibrium from time zero. This approach avoids initial blade model transients under starting rotation and prior to bird impact.

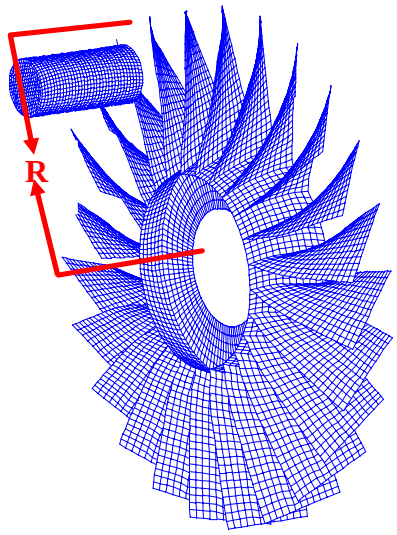

Figure 2 Bird impact location before impact

Material Property

Equation of state polynomial is used to define the property of bird considered to be hydrodynamic in nature having bulk modulus of K= 2.1 GPa with density 1050 kg/m^3. Figure 3 illustrates variation in compressibility of water with pressure. The constants in the polynomial equation of state have been obtained for a water air ratio of 90%.

Blade

The material property of bladed disc assembly is taken as that of titanium Ti-64 and following bilinear material property has been taken for transient dynamic analysis of bird impact.

Density	ρ	= 4420 kg/m^3
Young's Modulus	E	= 119.35 GPa
Hardening Modulus	E_h	= 0.959 GPa
Yield stress	σ_y	= 1311 MPa
Poisson's ratio	μ	= 0.3

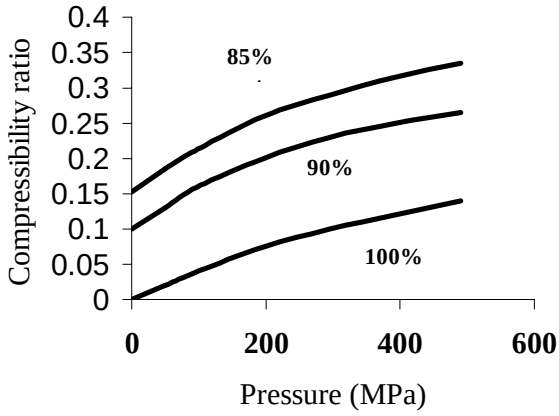

Figure 3 Material properties of the bird for different compressibility ratio

Boundary Conditions and Loads

Disc assembly is restrained in axial direction at the bore of the disc. Rotating speed of the disc and initial velocity of the bird are two initial boundary conditions. Rotating speed of the disc is taken as approximately 11000 rpm and axial velocity of the bird around 140 m/sec.

RESULTS AND DISCUSSION

A fully nonlinear analysis, including the effect of centrifugal stiffening, was conducted up to 3000 μs with the time step of one microsecond. Bird is associated with translation kinetic energy of 778.5 kJoule at 140-m/sec bird speed. Kinetic energy due to rotation of bladed disc assembly is 694.35 kJoule with 12.471-kJoule internal energy. As per the well known law of conservation of energy, sum total of energies should remain constant at any interval of time. However, with the explicit code there is loss of energy due to hourglass mode. In this analysis this

energy is always kept lower than 5% of the total input energy, for accurate output results.

Figures 4 and 5 show deformed plot of bladed disc assembly after bird impact at 1.7 and 2.8 milliseconds respectively. Deformed geometry of blades agrees with images captured from high-speed photography in bird impact test rig.

Bird impact leads to tearing of the blade but it is difficult to predict blade failure based on effective strain criterion. Forming limit diagram (FLD) concept is used to predict failure of blade due to bird impact. Blade failure criterion is predicted based on major and minor principal strain-contour locus at high strain rates.

The strain rate, pertinent to soft foreign-object impacts determined with real-blade bench impact tests performed by Bertke (1982) approaches 400 mm/mm/s. Tensile bar testing at low, intermediate, and high strain rates (range varying from 100 to 1000 mm./mm./s) performed by Emery (1998) indicates that the failure boundary strain value decreases with increasing strain rates. Forming limit diagrams at high and low strain rate for titanium are shown in Figures 8 and 10.

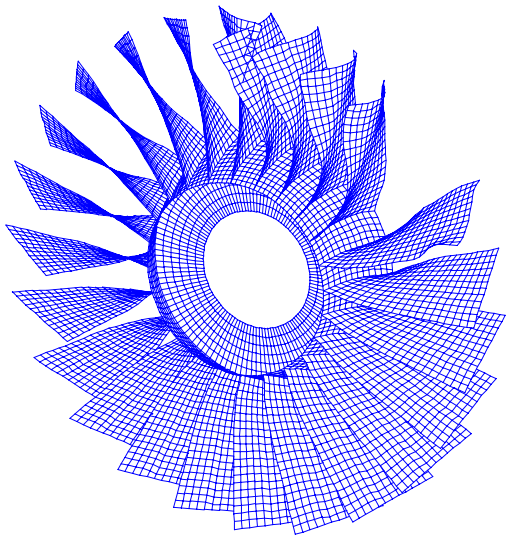

Figure 4 Blade deformation after 1.7 milli-seconds

The peak strain occurs on the suction side at the leading edge as shown in Figure 6. Figures 7 and 8 show the time history of the principal strains at location A and B indicated in Figure 6. In the present investigation these two locations are highly critical and have been selected after comparing fifty-six graphs of major and minor strain in all the six blades. Figure 7 indicates that after 220 μs, maximum and minimum principal strains are 0.071 and 0.043 respectively. Forming limit diagrams for titanium at high and low strain rate shown in Figure 8 are compared with loci of principal major and minor strains. This figure further reveals that at location **A** locus of major and minor strain do not cross strain damage boundary and hence blade will not fail or tear at this location and this agrees with the test results. Similarly, Figure 9 shows temporal plot of major and minor principal strain at location **B** shown in Figure 6. Figure 10 again indicates that loci of major and minor principal strain lies below the FLD boundary at high strain rate, indicating blade will also not tear at this location.

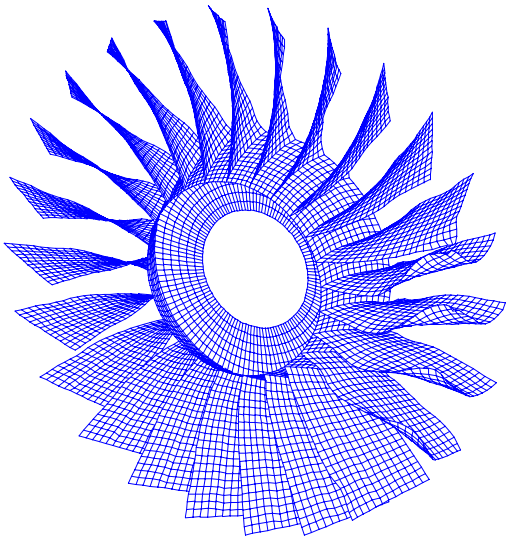

Figure 5 Blade deformation after 2.8 milli-seconds

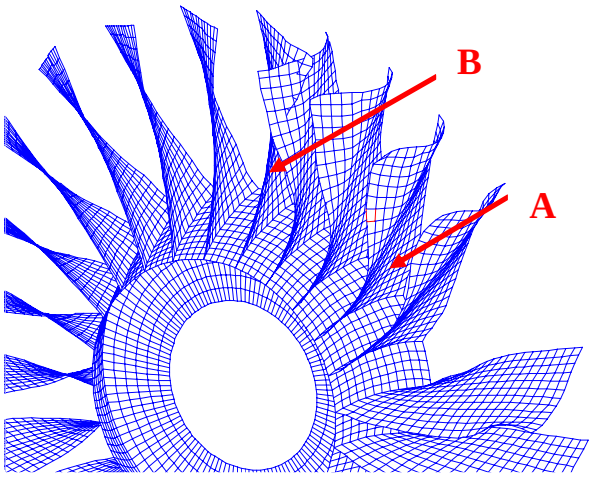

Figure 6 Critical locations of blade to predict blade failure

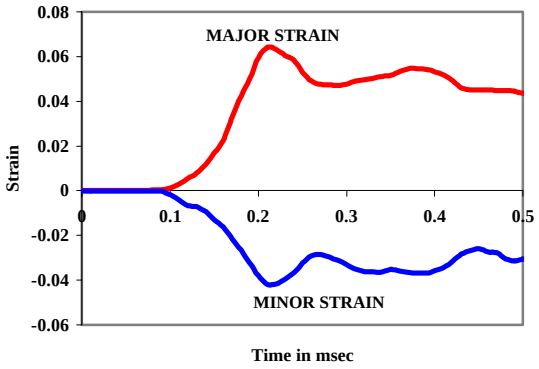

Figure 7 Temporal major and minor principal strain at location A

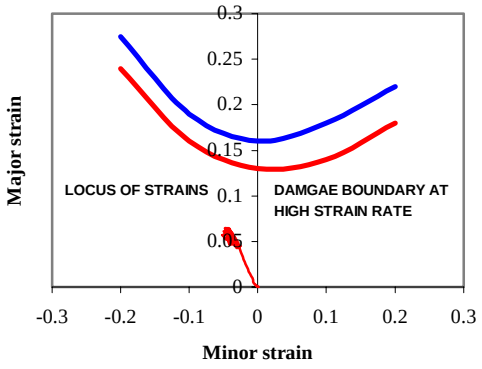

Figure 8 Major and minor principal strain with strain damage boundary at location A

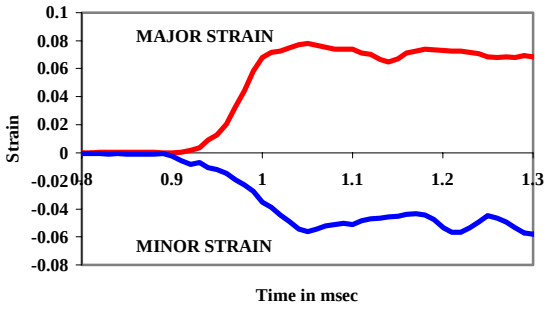

Figure 9 Temporal principal strains at location B

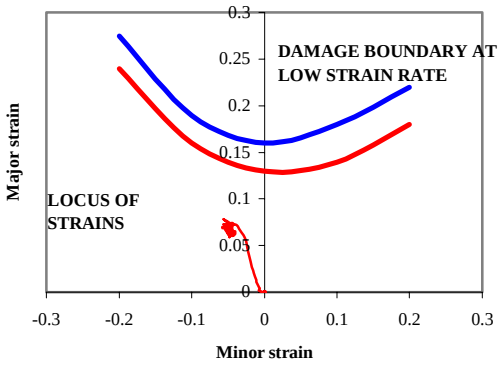

Figure 10 Major and minor principal strain with strain damage boundary at location B

Axial deflection is one of the other design constraints for designing bladed disc assembly against bird impact. Blades can strike stator blades both at the leading edge and trailing edge, which can lead to secondary failure of the rotating blades. Figures 11 and 12 show temporal variation in axial deflection in blade at the leading and trailing edge of the blade. These graphs show that the first blade has maximum forward axial deflection at the tip of leading and trailing edge and is equal to 32 and 8 mm respectively. Figure 11 further indicates that backward deflection in the trailing edge of this blade is 17-mm.

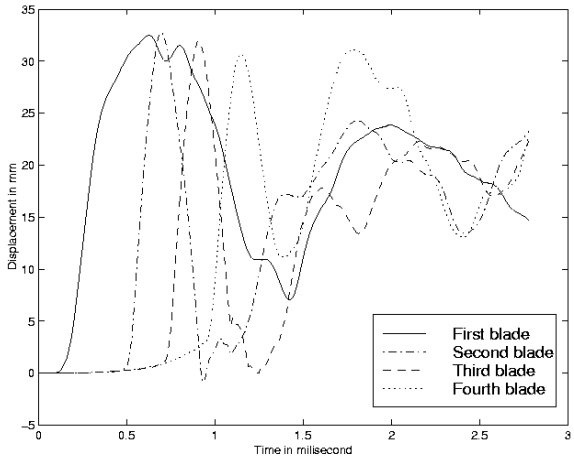

Figure 11 Dynamic axial deflection of blades at the leading edge

Experiments conducted on rotating fan bladed disc assembly show axial deflection of about 30 mm against numerical value of 32 mm at leading edge of bladed disc assembly in the forward direction showing a discrepancy of 6% against experimental value. Also trailing edge blade tip deflects by 17 mm

in the backward direction against numerical value of 24.6 mm. These two results show that numerical and experimental values match well with the analysis.

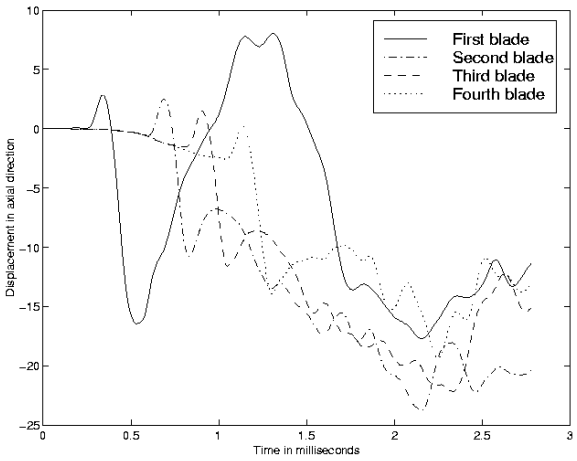

Figure 12 Dynamic axial deflection of blades at the trailing edge

Another important information from this analysis is the variation of axial thrust force with time. Figure 13 shows variation in axial force due to bird strike. This figure shows that maximum value of axial force is -42 kN around 0.5 mili-sec which match closely with the result obtained using Newton's second law of motion. Since, approximately 1/3rd of 0.9 kg bird mass strikes one rotating blade for 1 milli-seconds, therefore force exerted on bladed disc assembly for one blade is also 42 kN. Earlier, Ramachandra et al. (1996) evaluated transient engine bearing load using solid brick elements and obtained similar results.

This impact analysis also enables the estimation of unbalance forces on the bearing by calculating shift in center of gravity of bladed disc assembly during the impact phase. Figure 14 shows variation in unbalance force in the bladed disc assembly at the plane of the disc due to large deformation of the blades. This figure indicates that maximum unbalance force is 72 kN after two milliseconds. As per certification criterion disc assembly should have the capability to withstand unbalance load due to single blade-off situation. In this fan disc assembly, unbalance force due to single blade is 132kN, which is 35% greater than the maximum unbalance force due to bird strike.

CONCLUSIONS

A transient explicit, material and geometric nonlinear, FE-based impact analysis, MSC/DYTRAN, has been carried out to predict fan bladed disc capability to withstand 0.9 kg bird impact at critical flight condition. Numerical analysis indicates that blades do not tear based on forming limit diagram failure criterion which agrees well with the experimental test conducted during testing of fan rotor assembly in the experimental rig. Axial and radial deflection in the forward and backward direction matches very closely with the experimental value. This investigation further indicates that bird impact load leads to transient axial force in the forward direction, which should be taken, into account while designing axial thrust bearing. Large deformation due to bird strike on rotating blades results in radial unbalance force, which is lower than blade-off load in a disc assembly.

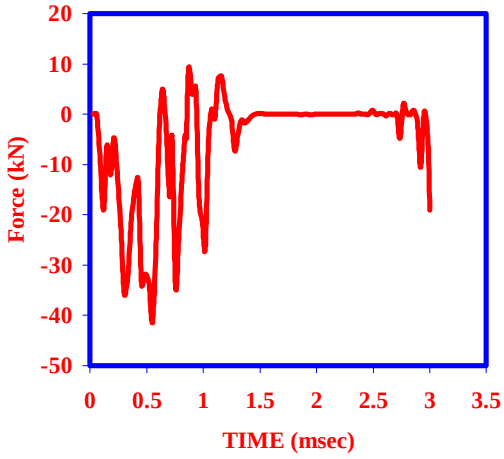

Figure 13 Axial thrust due to bird impact at critical flight velocity of the bird

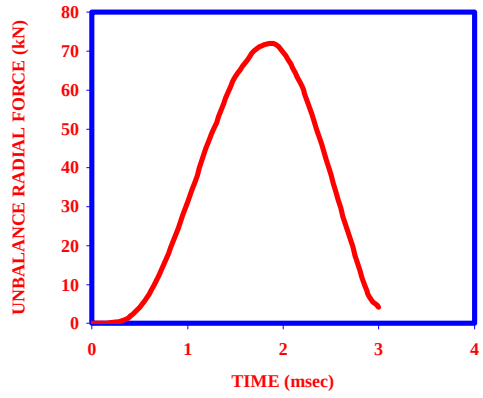

Figure 14 Unbalance force due to bird impact on rotating bladed disc assembly

ACKNOWLEDGEMENT

Authors are thankful to Mr. S. C. Kaushal, Director, Gas Turbine Research Establishment, Bangalore, India for giving permission to present this paper.

REFERENCES

Allock, A. W. R. and Collin, D. M., 1968, "The Development of a Dummy Bird for use in Bird Strike Research", U. D. C. No. 598.2:621-757.

Bertke, R. S., 1982, "Structural Element and Real Blade Impact Testing", University of Dayton Research Institute Report, UDRI-TR-82-02. Contract F33615-77-C-5221.

Cornell, R. W., 1976, " Elementary three-dimensional Interactive Rotor Blade Impact Analysis," *ASME Journal of Engineering for Power, Vol. 98, pp. 480-486.*

Emery, S. A., 1998, "Material Characterisation, Part A, Mechanical Properties of Two Metals at several Strain Rates", University of Dayton Research Institute Report UDRI-TR-79-98, Contract F33615-77-C-5221.

Jain, R. (2000), "Critical Flight Velocity for Fan Blades Due to Bird Hit," *GTRE-Report No 0001 0002 00 00 013 001.*

Martin, N. F. Jr., 1990, "Nonlinear Finite Element Analysis to Predict Fan Blade Damage Soft Body Impact," *Journal of Propulsion*, Vol. 86, pp. 445-450.

MSC-DYTRAN, 1992, Users Manual, The Macneal-Schwendler Corporation, Colorado Boulevard, Los Angeles, CA 90041-1777, USA.

Niering, E., 1990, "Simulation of Bird Strikes on Turbine Engines", *Journal of Engineering for Gas Turbine and Power*, Vol. 112, pp. 573-578.

Peterson, R. L. and Barber, J. P. 1976, " Bird Impact Forces in Aircraft Windshield Design," Report #AFFDL-TR-75-150

Ramachandra, K., Jain, R. and Chandrasekaran, M., 1996, "Evaluation of Transient Engine Bearing-Loads Due to Bird Strikes", 23/67, Bird Strike Committee Europe, London.

Storace, A. F., Nimmer, R. P., and Ravenhall, R., 1983, "Analytical and Experimental Investigation of Bird Impact on Fan and Compressor Blading", AIAA Journal of Aircraft, Vol. 21, No. 7, Paper No 83-0954.

Teichman, H. C. and Tandros, R. N., 1991, "Analytical and Experimental Simulation of Fan Blade Behaviour and Damage under Bird Impact", *Transaction of ASME Journal of Engineering for Gas Turbine and Power*, Vol. 113, pp. 582.

Wilbeck, J. S. and Rand, J. L., 1981, "The Development of a Substitute Bird Model", A*SME Journal of Engineering for Gas Turbine and Power*, Vol. 103, pp. 725-730.